Satish K. Awasthi[1]
S. C. Shankaramma[1]
S. Raghothama[2]
P. Balaram[1]

[1] *Molecular Biophysics Unit, Indian Institute of Science, Bangalore 560 012, India*

[2] *Sophisticated Instruments Facility, Indian Institute of Science, Bangalore 560 012, India*

Received 29 November 1999; accepted 22 February 2000

Solvent-Induced β-Hairpin to Helix Conformational Transition in a Designed Peptide

Abstract: *An octapeptide containing a central —Aib–Gly– segment capable of adopting β-turn conformations compatible with both hairpin ($\beta_{II'}$ or $\beta_{I'}$) and helical (β_I) structures has been designed. The effect of solvent on the conformation of the peptide Boc–Leu–Val–Val–Aib–Gly–Leu–Val–Val–OMe (**VIII**; Boc: t-butyloxycarbonyl; OMe: methyl ester) has been investigated by NMR and CD spectroscopy. Peptide **VIII** adopts a well-defined β-hairpin conformation in solvents capable of hydrogen bonding like $(CD_3)_2SO$ and CD_3OH. In solvents that have a lower tendency to interact with backbone peptide groups, like $CDCl_3$ and CD_3CN, helical conformations predominate. Nuclear Overhauser effects between the backbone protons and solvent shielding of NH groups involved in cross-strand hydrogen bonding, backbone chemical shifts, and vicinal coupling constants provide further support for the conformational assignments in different solvents. Truncated peptides Boc–Val–Val–Aib–Gly–Leu–Val–Val–OMe (**VII**), Boc–Val–Val–Aib–Gly–Leu–Val–OMe (**VI**), and Boc–Val–Aib–Gly–Leu–OMe (**IV**) were studied in $CDCl_3$ and $(CD_3)_2SO$ by 500 MHz ^{1}H-NMR spectroscopy. Peptides **IV** and **VI** show no evidence for hairpin conformation in both the solvents. The three truncated peptides show a well-defined helical conformation in $CDCl_3$. In $(CD_3)_2SO$, peptide **VII** adopts a β-hairpin conformation. The results establish that peptides may be designed, which are poised to undergo a dramatic conformational transition.* © 2001 John Wiley & Sons, Inc. Biopolymers 58: 465–476, 2001

Keywords: *β-hairpin; helix; conformational transition; truncated peptides; nuclear Overhauser effects; backbone chemical shifts*

INTRODUCTION

Conformations of polypeptide chains are determined by subtle sequence and environmental effects. The α-helix and β-sheet are the two major elements of secondary structure, which have been widely studied in proteins[1–3] and synthetic peptides and polypeptides.[4–6] Conformational transitions between these

Correspondence to: P. Balaram; email: pb@mbu.iisc.ernet.in
Contract grant sponsor: Department of Biotechnology, India

two ordered states of polypeptide chains were initially observed in studies of synthetic homopolypeptides.[7,8] Subsequently, studies of helix to sheet transitions have acquired a new dimension because of the importance of such conformational changes in pathological conditions involving prion proteins[9,10] and Alzheimer's disease.[11] Several recent investigations have focused on helix to sheet interconversions in model synthetic peptides.[12–20] Most studies have been carried out using amphiphilic sequences in aqueous solvents.[12,13] Alteration in pH,[14–16] temperature,[17] salt or organic cosolvent concentration[14,16,18] or redox state[19,20] have been used to initiate the structural transition, presumably by modulation of several distinct interactions involving both the polypeptide backbone and amino acid side chains.

We have been interested in designing an apolar peptide with a tendency to populate both well-defined helical and β-hairpin conformations, which would permit studies of conformational interconversion by varying the nature of organic solvent media. Structural transitions would be governed predominantly by the hydrogen-bonding ability of the solvent. We describe in this report conformational analysis of an apolar octapeptide Boc–Leu–Val–Val–Aib–Gly–Leu–Val–Val–OMe (**VIII**), which demonstrates solvent dependent conformational variability. The conformational analysis of the truncated peptides, Boc–Val–Val–Aib–Gly–Leu–Val–Val–OMe (**VII**), Boc–Val–Val–Aib–Gly–Leu–Val–OMe (**VI**), and Boc–Val–Aib–Gly–Leu–OMe (**IV**) were also studied (peptide numbers correspond to the number of residues). Evidence is presented for both helical and β-hairpin conformations.

EXPERIMENTAL PROCEDURE

Materials and Methods

Peptides were synthesized by classical solution phase procedures using a fragment condensation strategy described earlier.[21] The *t*-butyloxycarbonyl (Boc) group was used for N-terminal protection and the C-terminal was protected as a methyl ester (OMe). Deprotection was achieved with 98% formic acid or 2N NaOH/MeOH, respectively. Couplings were mediated by dicyclohexylcarbodiimide/1-hydroxybenzotriazole. All intermediates were characterized by ^{1}H-nmr (80 MHz) and thin layer chromatography on silica gel. These intermediates were used without further purification. Peptides were purified by medium pressure liquid chromatography on a C-18 (40–60 μ) column using methanol–water gradients. Peptides IV, VI, VII, and VIII were purified by high performance liquid chromatography on reverse phase (RP-HPLC) C-18 (10 μ) column using methanol–water gradients. The peptides were checked for homogeneity by analytical RP-HPLC (C-18, 250 $\times$ 4.6 mm, 5 μ) with a gradient of 60–95% aqueous methanol in 30 min; detection 226 nm, flow rate 0.8mL/min. Retention times (t_R min) were compared for the peptides under identical conditions. The peptides were characterized by complete assignment of ^{1}H-NMR spectra recorded on a Bruker DRX-500 MHz spectrometer and by electrospray mass spectrometry. The mass spectra were recorded on a HP 1100 electrospray ionization–mass spectroscopy (ESI-MS), interfaced with an HPLC. Data in the positive ion mode were acquired in the scan mode in the range of 200–1000 Da. Peptides were infused into the electrospray chamber in methanol solution using a flow of 0.04 mL/min.

Physical Data for Peptides VIII, VII, VI, and IV

***Boc–Leu–Val–Val–Aib–Gly–Leu–Val–Val–OMe* (VIII).** Melting point 116–118°C, t_R 20.8 min, ESI-MS: (calc. mass 896.6) 919($[M+Na]^+$), 897($[M+1]^+$).

Boc–Val–Val–Aib–Gly–Leu–Val–Val–OMe (VII). Melting point 120–122°C, t_R 17.8 min, ESI-MS: (calc. mass 783.5) 806($[M+Na]^+$), 784($[M+1]^+$).

Boc–Val–Val–Aib–Gly–Leu–Val–OMe (VI). Melting point 113–114°C, t_R 14.3 min, ESI-MS: (calc. mass 684.4) 707($[M+Na]^+$), 685($[M+1]^+$).

Boc–Val–Aib–Gly–Leu–OMe (IV). Melting point 101–103°C, t_R 12.1 min, ESI-MS: (calc. mass 486.3) 509($[M+Na]^+$), 487($[M+1]^+$).

NMR and CD

Resonance assignments were done using rotating frame nuclear Overhauser effect spectroscopy (ROESY) spectra. All two-dimensional experiments were recorded in phase sensitive mode by using the time proportional phase incrementation method. The amount of 1024 and 512 data points were used in the t_2 and t_1 dimensions, respectively. The resultant data set was zero filled to finally yield 1K $\times$ 1K data points. A shifted square sine bell window was used in both dimensions. Spectral widths were in the range of 4500 Hz. Peptide concentrations were $\sim$7 m*M* in $CDCl_3$, $(CD_3)_2SO$, and CD_3OH and 3 m*M* in CD_3CN. The probe temperature was maintained at 298K. CD spectra were recorded on JASCO J-500 spectropolarimeter using 1 mm path-length cells. Each spectrum is the resultant of four scans. Band intensities are reported as molar ellipticities, $[\theta]_M$ (deg cm^2 decimol^{-1}).

RESULTS AND DISCUSSION

Design

Peptide **VIII** was designed on the basis of earlier studies of peptide in this laboratory, which established

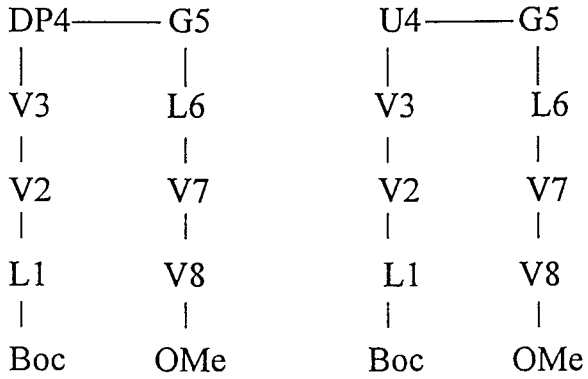

FIGURE 1 Schematic diagram of a two-residue loop β-hairpin conformation for octapeptides **BH8** (left) and **VIII** (right) respectively. U: Aib.

a β-hairpin conformation for the peptide Boc–Leu–Val–Val–D-Pro–Gly–Leu–Val–Val–OMe (**BH8)** in solution[22,23] and in crystals[24] (Figure 1). In peptide **BH8,** the D-Pro–Gly segment adopts a type II′ β-turn conformation, as a consequence of the restriction of ϕ D-Pro to a value $\sim +60° \pm 20°$. The type II′ β-turn serves as a nucleus for a hairpin conformation, which is further facilitated by the incorporation of the β-branched residue, valine, in the potential strand segment.[25,26] In peptide **VIII**, the D-Pro residue is replaced by Aib. Extensive stereochemical studies on achiral Aib residues have established a strong tendency to adopt either right-handed or left-handed ($\phi = 60° \pm 20°$, $\psi = 30° \pm 20°$) helical conformations.[27–32] In addition, theoretical calculations show the presence of minima in a semiextended region of ϕ,ψ space ($\phi = \pm 60° \pm 20°$, $\psi = \pm 120° \pm 20$).[27]

In peptide **VIII,** if Aib(4) adopts an α_L conformation, the Aib–Gly segment could adopt, in principle, a type I′ β-turn structure (ϕ Aib $\sim \phi$ Gly $\sim +60°$, ψ Aib $\sim \psi$ Gly $\sim +30°$) capable of nucleating a β-hairpin. If Aib(4) adopts a semiextended conformation ($\phi \sim \pm 60°$, $\psi \sim +120°$), the Aib–Gly segment can adopt a type II′ conformation analogous to peptide **BH8**.[22–24] However, it should be noted that the semiextended conformation is quite uncommon for Aib residues that are in an internal position in a peptide. A rare example of a type II′ Aib–Ala β-turn, with a semiextended Aib conformation has been observed in crystals of a cyclic hexapeptide having a disulfide linkage.[33] If Aib(4) adopts a right-handed helical conformation (α_R , $\phi \sim \pm 60°$, $\psi \sim \pm 30°$), then nucleation of a $3_{10}/\alpha$-helix over the entire length of sequence is possible. Indeed, several examples exist in the literature in which a single, centrally placed Aib residue nucleates a $3_{10}/\alpha$-helical conformation in peptides of length 7–8 residues.[27–31,34–36] The sequence of peptide **VIII** is set up to undergo conformational changes, with the Aib–Gly segment acting as a nucleus capable of adopting distinct conformational states. Figure 2 schematically illustrates

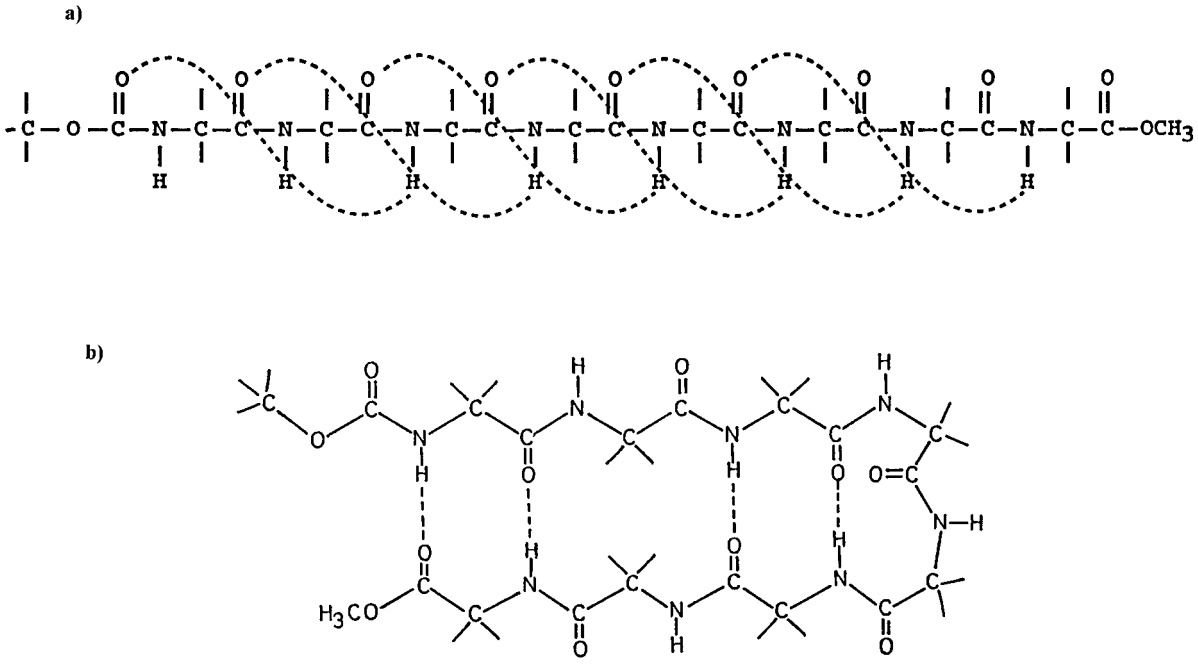

FIGURE 2 Schematic representation of intramolecular hydrogen bond patterns in ideal 3_{10}-helical and β-hairpin conformations.

the nature of intramolecular hydrogen-bond patterns anticipated in ideal 3_{10}-helical and β-hairpin conformations of the protected octapeptide. In the 3_{10}-helix, 6 intramolecular hydrogen bonds are possible, while in the β-hairpin a maximum of four intramolecular hydrogen bonds are possible. Clearly, if there are no overwhelming preferences for specific local backbone conformation at individual residues (barring Aib) then overall peptide conformation may indeed be driven by the balance between intrapeptide and solvent-peptide hydrogen bonds. Consideration of a 3_{10}-helix is reasonable because many small Aib-containing peptides do indeed adopt 3_{10}-helical folds.[27,34,37–39] Furthermore, even in cases where mixed $3_{10}/\alpha$-helical structures are observed, the initial turn at the N-terminus accommodates both $4 \rightarrow 1$ and $5 \rightarrow 1$ hydrogen bonds, resulting in only two non hydrogen-bonded NH groups at the amino terminus end.[34]

Circular Dichroism

Figure 3a shows the CD spectra of **VIII** in methanol and acetonitrile. Two distinct bands at 204 and 219 nm are observed in acetonitrile, characteristic of a significant population of helical conformations. The CD spectra resemble those observed earlier for short helical peptides in organic solvents.[40,41] In sharp contrast, in methanol, a single negative band at 215 nm, is observed, a feature that has also been noticed in several short peptides adopting a β-hairpin conformation.[22,23,42–45] The solvent dependence of CD spectra suggests that conformer populations are biased in favor of helical structures in a solvent like acetonitrile, which has a limited ability to hydrogen bond with peptides, since it is capable of acting as a hydrogen acceptor. In methanol, which can, in principle, act as both hydrogen donor and acceptor, β-hairpin conformations appear to predominate. Based on these observations, detailed NMR studies were undertaken in four solvents $CDCl_3$, CD_3CN, CD_3OH, and $(CD_3)_2SO$. CD spectra of truncated peptides **VII**, **VI,** and **IV** are shown in Figure 3b. Despite loss of Leu(1), the CD spectrum of peptide **VII** in methanol shows evidence for the presence of a significant population of β-hairpin conformers. Further truncation of the sequence results in a loss of ellipticity at 215 nm. Nuclear magnetic resonance analysis of shorter peptides (vide infra) reveals no evidence for putative hairpin conformations.

NMR Analysis

Peptide **VIII** exhibited sharp well-resolved 500 MHz ^{1}H-NMR spectra in all four solvents. Complete resonance assignments were readily achieved using

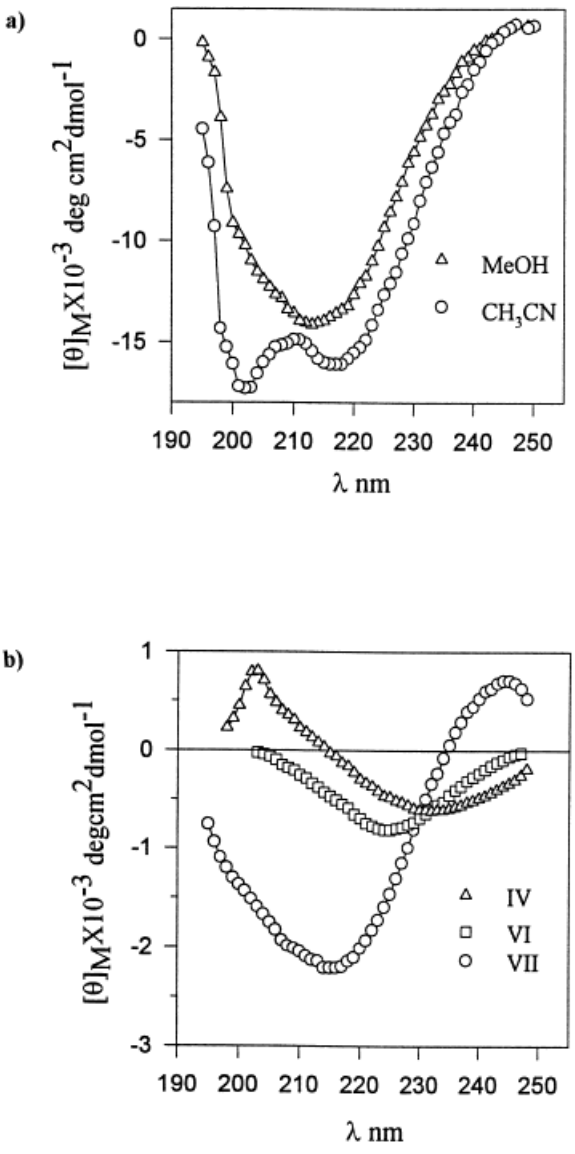

FIGURE 3 CD spectra of peptides **VIII**, **VII**, **VI**, and **IV**. (a) Peptide **VIII** in methanol (△) and in acetonitrile (○). (b) Peptides **VII**, **VI**, and **IV** in methanol. Concentration of the peptides: $\sim 2.7 \times 10^{-4}$ mmol.

ROESY spectra and specific features of one-dimensional (1D) spectra—viz. multiplicity of Aib (singlet) and Gly (triplet) NH resonances that facilitate unambiguous assignments. The chemical shifts of the backbone NH and $C^{\alpha}H$ protons in the four solvents are summarized in Figure 4. Chemical shifts of $C^{\alpha}H$ and NH protons are a very sensitive indicator of backbone conformation in polypeptides.[46–48] It is readily apparent from Figure 4 that the chemical shift patterns observed in $CDCl_3$ and CD_3OH are distinctly different. In $CDCl_3$, all NH protons appear distinctly upfield relative to the positions in CD_3OH. The $C^{\alpha}H$ protons show a significantly larger chemical shift dispersion in CD_3OH as compared to $CDCl_3$. The

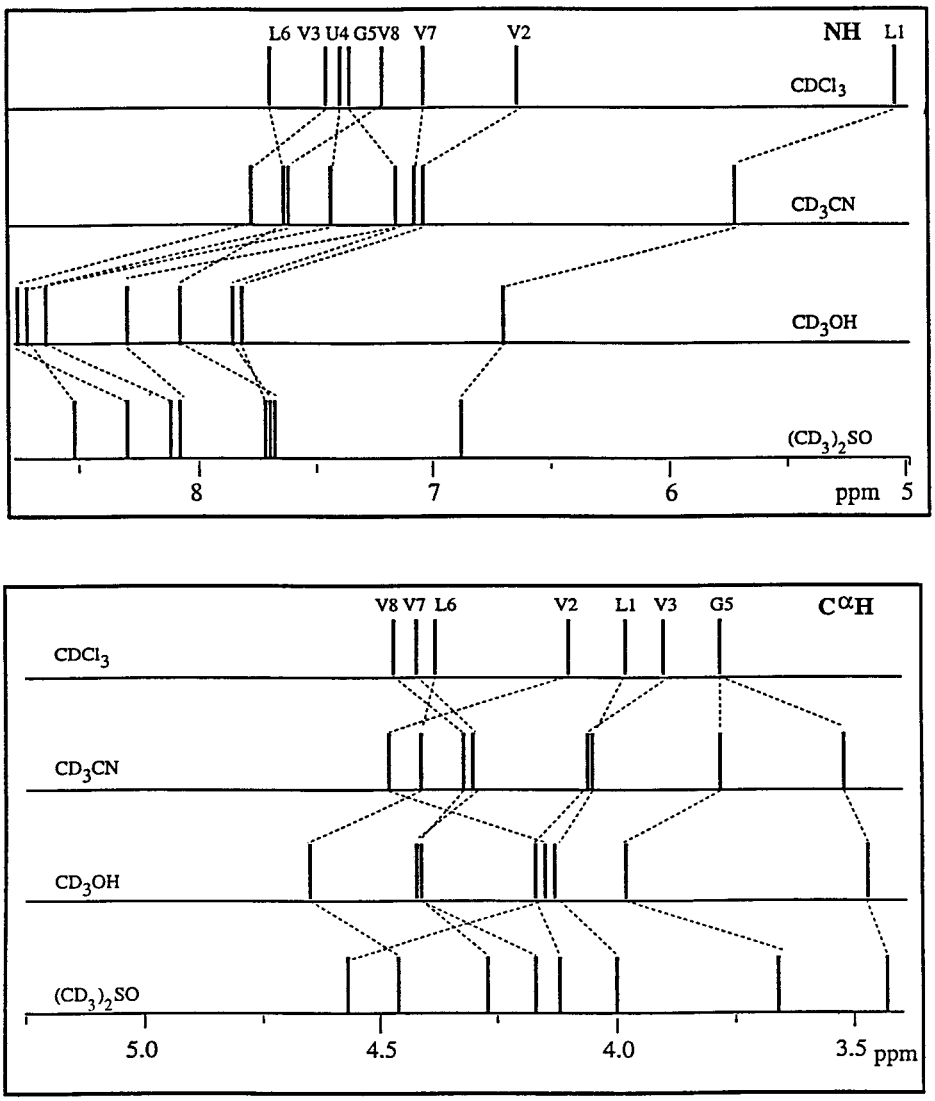

FIGURE 4 Schematic representation of NH and $C^{\alpha}H$ chemical shifts for peptide **VIII** in $CDCl_3$, CD_3CN, $(CD_3)_2SO$, and CD_3OH.

solvent dependence of chemical shifts, particularly of $C^{\alpha}H$ protons, which do not interact strongly with a hydrogen-bonding solvent, is a clear indicator of shifting conformer populations. Nuclear Overhauser effects[49] that are of specific importance in conformational assignments are summarized in Table I.

Conformations in $(CD_3)_2SO$

In $(CD_3)_2SO$, a strong NOE is observed between Val(2)$C^{\alpha}H$ ↔ Val(7)$C^{\alpha}H$, clearly diagnostic of a β-hairpin structure (Figure 5). The presence of strong sequential $C^{\alpha}{}_iH \leftrightarrow N_{i+1}H$ NOEs from Leu(1) to Aib(4) and Gly(5) to Val(8) and absence of sequential NH ↔ NH connectivity over the segment Val(2) ↔ Val(8) (Figure 6) support a major population of β-hairpins. The large $^3J_{NH\text{-}C^{\alpha}H}$ values for the Leu(1) ↔ Val(3) [Leu(1) 9.1 Hz, Val(2) 9.6 Hz, Val(3) 8.2 Hz] segment also support the β-strand conformation, although somewhat lower values are detected for the C-terminus [Leu(6) 5.6 Hz, Val(7) 7.1 Hz, Val(8) 7.8 Hz]. The pattern of $C^{\alpha}H$ and NH chemical shifts for peptide **VIII** in $(CD_3)_2SO$ closely parallels that observed for the parent β-hairpin model **BH8**, which contains D-Pro in place of Aib(4).

Conformations in CD_3OH

From Table I, two key long-range NH ↔ NH NOEs Leu(1) ↔ Val(8) and Val(3) ↔ Leu(6) are evident. These cross-strand NOEs provide clear evidence for an appreciable population of β-hairpins. The rela-

Table I Summary of NOEs for the Peptides in $CDCl_3$ and $(CD_3)_2SO$

	Summary of NOEs[a]					
	NH↔NH		$C^{\alpha}H \leftrightarrow NH$		Conformational Conclusions	
	$CDCl_3$	DMSO	$CDCl_3$	DMSO	$CDCl_3$	DMSO
Peptide **VIII**						
L(1) ↔ V(2)	w (s)	m [s]	s (s)	s [m]		
V(2) ↔ V(3)	w (w)	— [—]	m (s)	s [m]	Helix	Hairpin
V(3) ↔ U(4)	— (m)	—	— (s)	s [m]	(major)	(major)
U(4) ↔ G(5)	— (m)	— [s]	— (—)	— [—]		
G(5) ↔ L(6)	s (s)	— [m]	w (w)	s [m]	Hairpin	Helix
L(6) ↔ V(7)	s (s)	— [m]	s (s)	s [s]	(minor)	(minor)
V(7) ↔ V(8)	m (m)	— [—]	s (s)	s [s]		
					$C^{\alpha}H \leftrightarrow C^{\alpha}H$ NOEs	
V(2) ↔ V(7)					m (m)	s
L(1) ↔ V(8)	— (w)	— [w]				
V(3) ↔ L(6)	— (w)	[s]				
Peptide **VII**						
V(1) ↔ V(2)	w	w	s	s		
V(1) ↔ U(3)	w	w	s	s	Helix	Hairpin
U(3) ↔ G(4)	m	m	—	—	(major)	(major)
G(4) ↔ L(5)	s	—	w	s		
L(5) ↔ V(6)	s	w	s	s		
V(6) ↔ V(7)	m	—	s	s		
					$C^{\alpha}H \leftrightarrow C^{\alpha}H$ NOEs	
V(1) ↔ V(6)					—	m
Peptide **VI**						
V(1) ↔ V(2)	s	s	m	m		
V(2) ↔ U(3)	s	s	m	m		
U(3) ↔ G(4)	m	s	—	—	Helix	Helix
G(4) ↔ L(5)	m	m	w	m		
L(5) ↔ V(6)	m	s	m	m		
Peptide **IV**						
V(1) ↔ U(2)	w	m	s	m		
U(2) ↔ G(3)	s	—	—	—	Turn	Turn
G(3) ↔ L(4)	m	—	m	s		
V(1) ↔ L(4)	—	w				

[a] NOEs of peptide **VIII** in CD_3CN and CD_3OH are given in parentheses and square brackets, respectively. NOE intensities are abbreviated as s = strong; m = medium; w = weak; — indicates that no NOE was detectable under the conditions used.

tively intense $C_i^{\alpha}H \leftrightarrow N_{i+1}H$ NOEs are also consistent with extended conformations for the Leu(1) to Val(3) and Leu(6) to Val(8) segments. Large $^3J_{NH\text{-}C^{\alpha}H}$ coupling constant (>8 Hz) are also observed for the residues in the strand segment, with the exception of Val(2). Cross strand Val(2) $C^{\alpha}H \leftrightarrow$ Val(7) $C^{\alpha}H$ NOEs are not observed because of overlap and interference from the residual OH signal in CD_3OH. The Aib(4) ↔ Gly(5) and Gly(5) ↔ Leu(6) N_i H($N_{i+1}H$ NOEs are consistent with a local helical conformation at Aib(4) and Gly(5), suggestive of a type I′ β-turn structure at this segment [Aib(4) $\phi = 60°$, $\psi = 30°$; Gly(5) $\phi = 90°$, $\psi = 0°$]. The absence of detectable sequential NH ↔ NH NOEs in the Val(2) ↔ Aib(4) and Val(7) ↔ Val(8) segments is indicative of an absence of a significant population of continuous helical conformations. The observation of the sequential NH ↔ NH NOEs between Leu(1) ↔ Val(2) and Leu(6) ↔ Val(7) does suggest, however, that there is conformational heterogeneity in solution, with the possibility of structures in which Leu(1) and Leu(6) lie in the helical region of ϕ,ψ space. The body of NMR evidence favors a predominance of β-hairpin conformations in CD_3OH, consistent with the conclusions drawn from the CD spectra in Figure 3a.

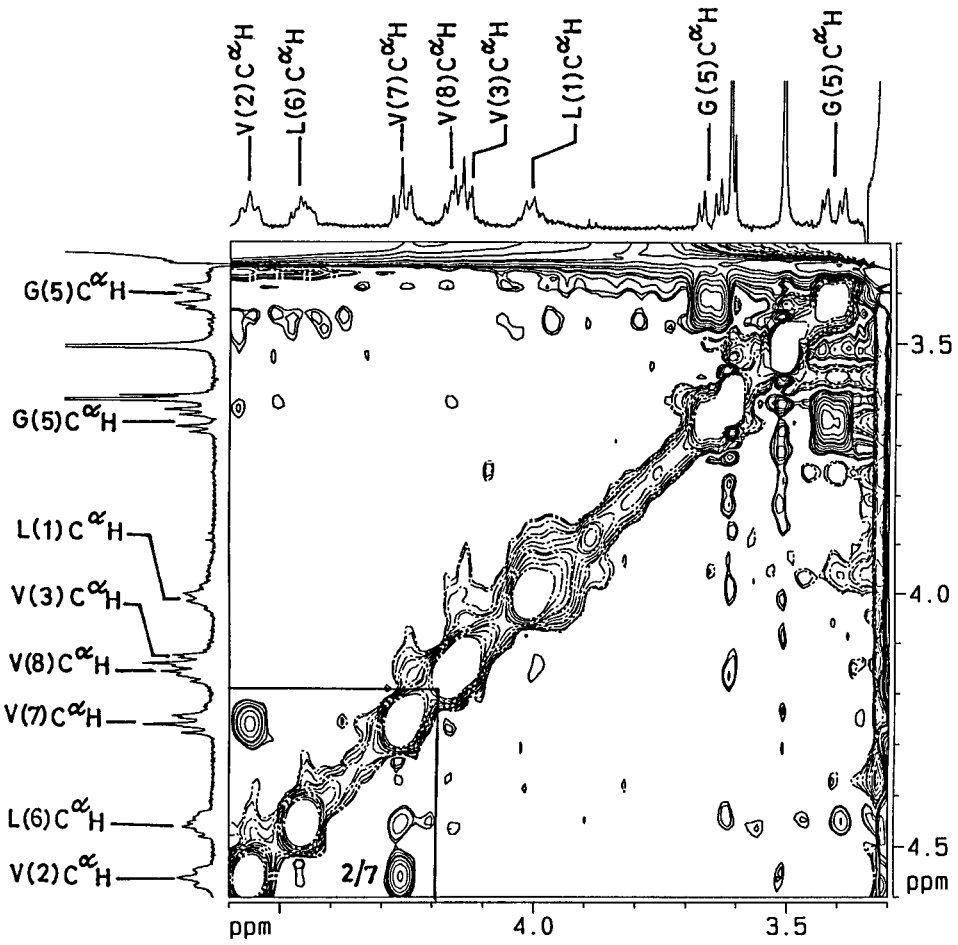

FIGURE 5 Partial ROESY spectrum of the peptide **VIII** in $(CD_3)_2SO$ highlighting $C^{\alpha}H \leftrightarrow C^{\alpha}H$ cross strand NOEs.

Conformations in $CDCl_3$

In this solvent, the pattern of NOEs (Table I) is suggestive of population of both helical and β-hairpin conformations, although sequential $N_iH \leftrightarrow N_{i+1}H$ NOEs are not observed (Figures 7 and 8) over the entire peptide length. The comparison of chemical shifts observed for peptide **VIII** with the parent β-hairpin **BH8** reveals several important differences. The much smaller dispersion of both NH and $C^{\alpha}H$ chemical shifts in peptide **VIII** suggests that β-hairpin conformations are only minor contributors to the conformational equilibrium. The largest chemical shift difference between **VIII** and **BH8** are observed for Val(3) NH (1.26 ppm), Gly(5) NH (1.25 ppm), Val(8) NH (1.11 ppm), Val(2) $C^{\alpha}H$ (0.64 ppm), Val(3) $C^{\alpha}H$ (0.64 ppm). The observed $^3J_{NCH^{\alpha}H}$ values at Val(2), Val(3), and Leu(6) are also much lower [Val(2) 4.7 Hz, Val(3) 4.9 Hz, and Leu(6) 6.9 Hz] , characteristic of helical conformations.

Addition of the free radical 2,2,6,6 tetramethylpiperidine-1-oxyl[50,51] (TEMPO) resulted in selective broadening of Leu(1) and to some extent Val(2) NH, while the remaining NH resonances were largely unaffected up to a radical concentration of 11.4 $\times$ $10^{-4}M$ (data not shown). This suggests greater solvent exposure of Leu(1) and Val(2) NH, a feature suggestive of a predominantly 3_{10} -helical conformation.

Conformations in CD_3CN

In this solvent three cross-strand NOEs diagnostic of β-hairpin conformations are observed—viz. Leu(1) NH $\leftrightarrow$ Val(8) NH, Val(3) NH $\leftrightarrow$ Leu(6) NH, and Val(2) $C^{\alpha}H \leftrightarrow$ Val(7) $C^{\alpha}H$ (Table I) . Of these, the two long- range NH $\leftrightarrow$ NH NOEs are very weak in intensity, suggestive of a relatively low population of folded hairpins. In contrast, to the results in CD_3OH and $(CD_3)_2SO$ sequential $N_iH \leftrightarrow N_{i+1}H$ are observed over the entire length of the peptide, strongly suggesting an appreciable population of helical conformations. The $^3J_{NCH^{\alpha}H}$ values for the Leu(1) to Val(3)

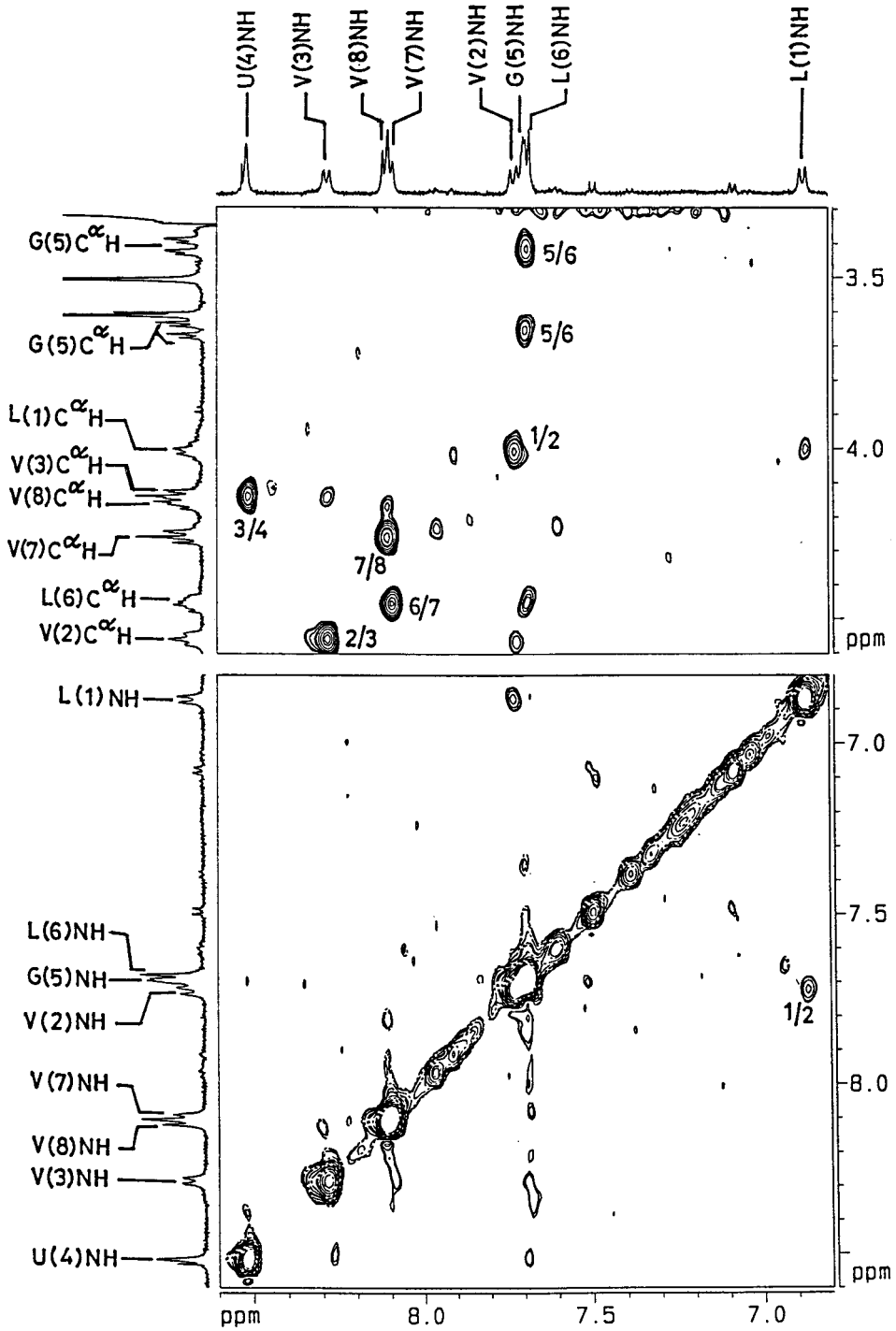

FIGURE 6 Partial ROESY spectra of peptide **VIII** in $(CD_3)_2SO$. The top panel shows $C^{\alpha}H$ ↔ NH NOEs, and the lower panel shows NH ↔ NH NOEs. Assignments are marked on the 1D spectra.

segment [Leu(1) 6.3 Hz, Val(2) 8.5 Hz, Val(3) 7.0 Hz] are also appreciably lower than that determined in $(CD_3)_2SO$. The nmr data thus favors a major population of helical conformations in CD_3CN, consistent with the CD results (Figure 3a).

NMR Analysis of Truncated Peptides

Sequence-specific assignments in $CDCl_3$ and $(CD_3)_2SO$ were readily achieved for peptides **VII**, **VI,** and **IV**. The key interresidue NOEs between backbone protons are

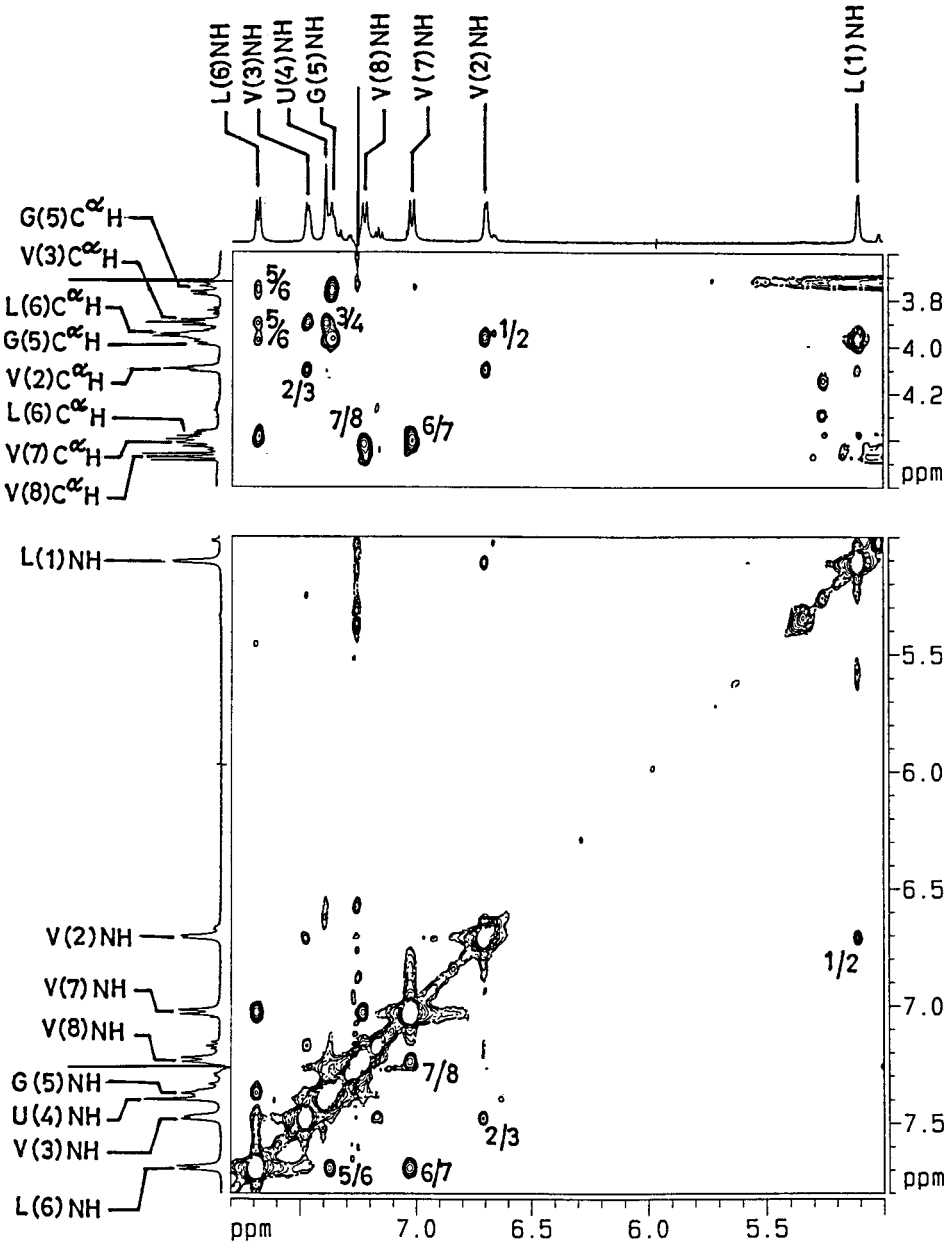

FIGURE 7 Partial ROESY spectra of peptide **VIII** in $CDCl_3$. The top panel shows $C^{\alpha}H \leftrightarrow NH$ NOEs, and the lower panel shows NH ↔ NH NOEs. Assignments are marked on the 1D spectra.

summarized in Table I. Interstrand NOEs characteristic of a population of β-hairpin conformations were observed only for peptide **VII** in $(CD_3)_2SO$. Figure 9 shows the ROESY spectra of peptide **VII**, illustrating the observed NOE between Val(1)$C^{\alpha}H$–Val(6)$C^{\alpha}H$. In all three truncated peptides, sequential NH—NH NOEs characteristic of local helical conformations are observed. The inference that largely helical conformations are favored in $CDCl_3$ for peptides **VII**, **VI**, and **IV** is consistent with the observed NOE results. The delineation of intramolecularly hydrogen-bonded NH groups in peptides **VII**, **VI**, and **IV** was achieved using solvent titration of NH chemical shifts in $CDCl_3$–$(CD_3)_2SO$ mixtures and free radical (TEMPO) induced broadening in $CDCl_3$. In all the three peptides, clear evidence was obtained for the solvent exposure of NH groups of residues 1 and 2 only (data not shown). These observations, together with the known tendency of Aib residues to promote helical folding in peptides, argue for a preponderance of helical conformations in peptides **VII**, **VI**, and **IV** in $CDCl_3$. Further support for this conclusion is obtained from the crystal structure of peptide **IV**, which reveals an incipient 3_{10}-helical conformation involving Gly(3)NH and Leu(4)NH in intramolecular hy-

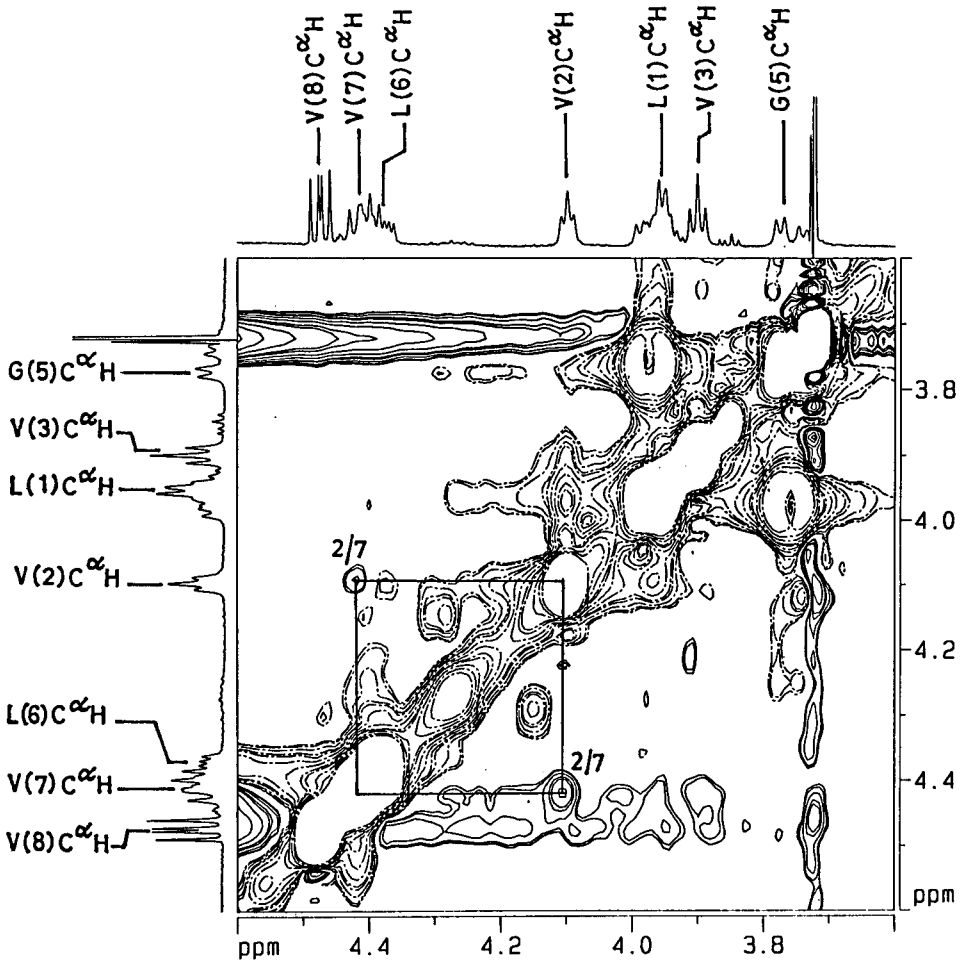

FIGURE 8 Partial ROESY spectrum of peptide **VIII** in $CDCl_3$, highlighting $C^{\alpha}H \leftrightarrow C^{\alpha}H$ cross-strand NOEs.

drogen bonds (N. Shamala, personal communication). In $(CD_3)_2SO$, helical conformations appear to persist in the case of peptides **IV** and **VI,** with no evidence obtained for short hairpin structures. However, in peptide **VII**, β-hairpin conformations make a significant contribution to the conformational equilibrium, as evidenced by the intense Val(1)$C^{\alpha}H$–Val(6)$C^{\alpha}H$ NOE.

CONCLUSIONS

The NMR and CD results presented in this paper suggest that the octapeptide Boc–Leu–Val–Val–Aib–Gly–Leu–Val–Val–OMe (**VIII)** is poised to undergo a solvent-dependent conformational transition between β-hairpin and 3_{10}-helical structures. In solvents capable of hydrogen bonding like $(CD_3)_2SO$ and CD_3OH, β-hairpins are favored. In the β-hairpin conformation, solvation of the CO and NH groups that face outward from the strand segments and the central peptide group in the β-turn is favored in solvents that can form hydrogen bonds. In particular, in methanol, both donor and acceptor interactions are possible, facilitating peptide bond solvation. In solvents that have a lower tendency to interact with backbone peptide groups, helical conformations are predominant. The balance between inter- and intramolecular hydrogen bonds determines the conformational distribution. In the present study, we have preferred to make an assignment of a 3_{10}-helical conformational in $CDCl_3$ based upon the observation of only two solvent-exposed NH groups in the nmr studies. In short peptides, with relatively low Aib content, α-helical conformations also have been observed in the solid state.[28–31] We have deliberately underemphasized the precise nature of the helical conformation since $3_{10}/\alpha$-helical and mixed helical structures can all be broadly grouped into one conformational family of peptide helices with very small barriers to interconversion amongst themselves.[52] The purpose of the present study is really to explore conformational interconver-

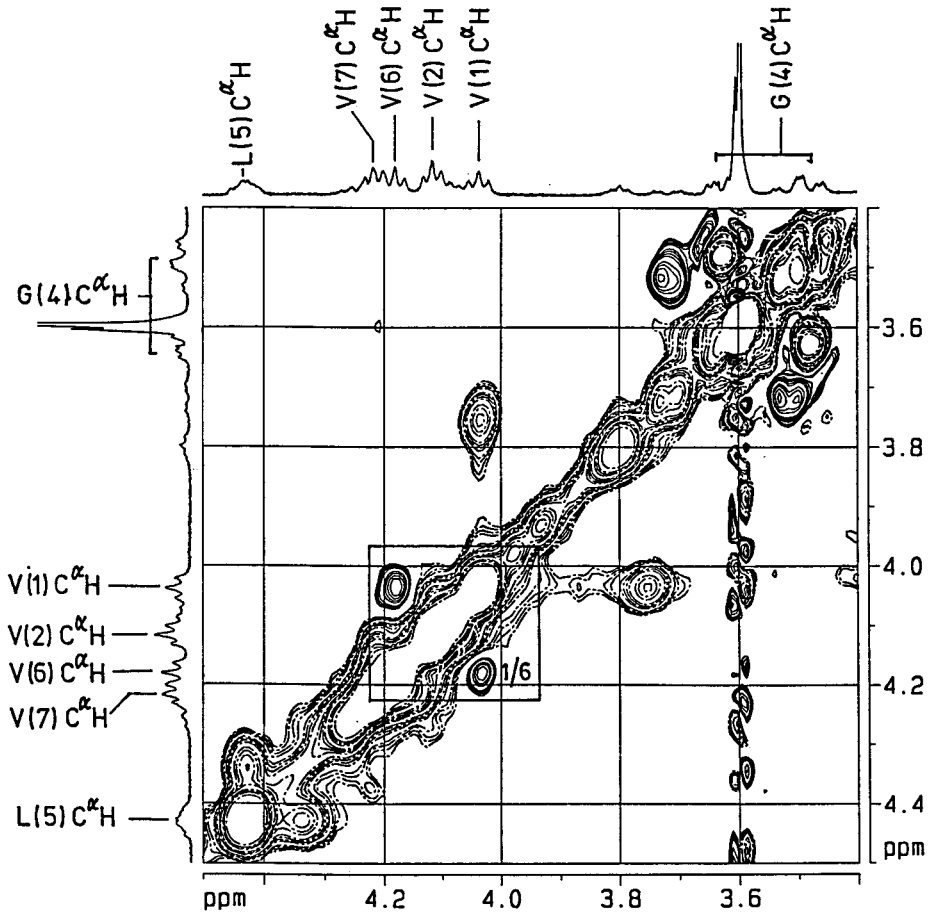

FIGURE 9 Partial ROESY spectrum of peptide **VII** in $(CD_3)_2SO$, highlighting $C^{\alpha}H \leftrightarrow C^{\alpha}H$ cross strand NOEs.

sion between families of the β-hairpin conformation on one hand and helices on the other.

The observation of sharp nmr resonances in all four solvents indicates that the rates of interconversion are fast on the nmr time scale. However, a low temperature study may indeed permit determination of activation barriers for such processes. Studies on truncated sequences suggest that chain length has a major influence on the equilibrium between β-hairpin and helical structures. In the shorter peptides, helices appear to predominate, while in the 7 and 8 residue peptides β-hairpins are populated under favorable solvent conditions. This study also illustrates the possibility of selectively using Aib residues to nucleate isolated turns in the context of non-helical structures, resulting in stabilization of β-hairpins in an acyclic peptide. An earlier example of a β-hairpin containing a Aib residue in the turn segment involved covalent cross-linking of antiparallel strands through disulfide linkages.[33] Several recent studies employ D-Pro–Xxx and Asn–Gly segments for nucleation of the β-hairpin conformations (see Ref. 29 and references cited therein). Our present study suggest that centrally positioned Aib–Gly segments may also serve to nucleate β-hairpins although these sequences may be more prone to conformational changes upon varying solvent composition. The use of D-residues in place of Gly may be an effective way of stabilizing hairpins over right-handed helical conformations.

SCS was supported by the award of a Research Associateship from the Council of Scientific and Industrial Research, India. Program support in the area of 'Drug and Molecular Design', Department of Biotechnology, India, is gratefully acknowledged.

REFERENCES

1. Richardson, J. S. Adv Protein Chem 1981, 34, 167–330.
2. Chothia, C.; Levitt, M.; Richardson, D. J Mol Biol 1981, 145, 215–250.
3. Richardson, J. S.; Richardson, D. C.; Tweedy, N. B.; Gernert, K. M.; Quinn, T. P.; Hecht, M. H.; Erickson, B. W.; Yan, Y.; McClain, R. D.; Dolan, M. E.; Surles, M. E. Biophys J 1992, 63, 1186–1209.
4. DeGrado, W. F. Adv Protein Chem 1988, 39, 51–124.

5. Richardson, J. S.; Richardson, D. C. Science 1988, 240, 1648–1652.
6. Rizo, J.; Gierasch, L. M. Ann Rev Biochem 1992, 61, 387–418.
7. Rosenheck, K.; Doty, P. Proc Natl Acad Sci USA 1961, 47, 1775–1785.
8. Greenfield, B.; Davidson, B.; Fasman, G. D. Biochemistry 1967, 6, 1630–1637.
9. Zhang, H.; Kaneko, K.; Nguyen, J. T.; Livshits, T. L.; Baldwin, M. A.; Cohen, F. E.; James, T. L.; Prusiner, S. B. J Mol Biol 1995, 250, 514–526.
10. Nguyen, J.; Baldwin, M. A.; Cohen, F. E.; Prusiner, S. B. Biochemistry 1995, 34, 4186–4192.
11. Kelly, J. W.; Lansbury P. T. Amyloid 1994, 1, 186–205.
12. Tuchscherer, G.; Grell, D.; Mathieu, M.; Mutter, M. J Pept Res 1999, 54, 185–194.
13. Mutter, M..; Hersperger, R. Angew Chem Int Ed Engl 1990, 29, 185–187.
14. Cerpa, R.; Cohen, F. E.; Kuntz, I. D. Folding Design 1996, 1, 91–101.
15. Mutter, M.; Gassmann, R.; Buttkus, U.; Altmann, K. H. Angew Chem Int Ed Eng 1991, 30,1514–1516.
16. Zhang, S.; Rich, A. Proc Natl Acad Sci USA 1997, 94, 23–28.
17. Fukushima, Y. Bull Chem Soc Jpn 1996, 69, 701–708.
18. Reed, J.; Kinzel, V. Biochemistry 1991, 30, 4521–4528.
19. Dado, G. P.; Gellman, S. H. J Am Chem Soc 1993, 115, 12609–12610.
20. Schenck, H. L.; Dado, G. P.; Gellman, S. H. J Am Chem Soc 1996, 118, 12487–12494.
21. Awasthi, S. K.; Raghothama, S.; Balaram, P. J Chem Soc Perkin Trans 2, 1996, 2701–2706.
22. Awasthi, S. K.; Raghothama, S.; Balaram, P. Biochem Biophys Res Commun 1995, 216, 375–381.
23. Raghothama, S.; Awasthi S. K.; Balaram, P. J Chem Soc Perkin Trans 2, 1998,137–143.
24. Karle, I. L.; Awasthi, S. K.; Balaram, P. Proc Natl Acad Sci USA 1996, 93, 8189–8193.
25. Sibanda, B. L.; Thornton, J. M. Nature (London) 1985, 316, 170–174.
26. Gunasekaran, K.; Ramakrishnan, C.; Balaram, P. Protein Eng 1997, 10, 1131–1141.
27. Prasad, B. V. V.; Balaram, P. CRC Crit Rev Biochem 1984, 16, 307–348.
28. Karle, I. L.; Balaram, P. Biochemistry 1990, 29, 6748–6755.
29. Kaul, R.; Balaram, P. Bioorg Med Chem 1999, 7, 105–117.
30. Toniolo, C.; Benedetti, E. Macromolecules 1991, 24, 4004–4009.
31. Toniolo, C.; Benedetti, E. ISI Atlas of Science: Biochemistry 1988, 255–230.
32. Marshall, G. R.; Hodgkin, E. E.; Langs, D. A.; Smith, G. D.; Zabrocki, J.; Leplawy, M. T. Proc Natl Acad Sci USA 1990, 87, 487–491.
33. Karle, I. L.; Kishore, R.; Raghothama, S.; Balaram, P. J Am Chem Soc 1988, 110, 1958–1963.
34. Karle, I. L.; Flippen-Anderson, J. L.; Gurunath, R.; Balaram, P. Protein Sci 1994, 4, 1547–1555.
35. Karle, I. L.; Flippen-Anderson, J. L.; Uma, K.; Balaram, P. Biopolymers 1993, 33, 827–837.
36. Banerjee, A.; Datta, S.; Pramanik, A.; Shamala, N.; Balaram, P. J Am Chem Soc 1996, 118, 9477–9483.
37. Bavoso, A.; Benedetti, E.; Di Blasio, B.; Pavone, V.; Toniolo, C.; Bonora, G. M. Proc Natl Acad Sci USA 1986, 83, 1988–1992.
38. Toniolo, C.; Benedetti, E. Trends Biochem Sci 1991,16, 350–353.
39. Datta, S.; Shamala, N.; Banerjee, A.; Pramanik, A.; Bhattacharjya, S.; Balaram, P. J Am Chem Soc 1997, 119, 9246–9251.
40. Sudha, T. S.; Vijaykumar, E. K. S.; Balaram, P. Int J Peptide Protein Res 1983, 22, 464–468.
41. Karle, I. L.; Flippen-Anderson, J. L.; Sukumar, M.; Uma, K.; Balaram, P. J Am Chem Soc 1991, 113, 3952–3956.
42. Alvarado, M. R.; Blanco, F. J.; Serrano, L. Nat Struct Biol 1996, 3, 604–612.
43. Nesloney, C. L.; Kelly, J. W. J Am Chem Soc 1996, 118, 5836–5845.
44. Schneider, J. P.; Kelly, J. W. J Am Chem Soc 1995, 117, 533–546.
45. Krause, E.; Beyermann, M.; Fabian, H.; Dathe, M.; Rothemund, S.; Bienert, M. Int J Peptide Protein Res 1996, 48, 559–568.
46. Wishart, D. S.; Sykes, B. D. Methods Enzymol 1994, 239, 363–392.
47. Wishart, D. S.; Sykes, B. D.; Richards, F. M. J Mol Biol 1991, 222, 311–333.
48. Wishart, D. S.; Bigam, C. G.; Holm, A.; Hodges, R. S.; Sykes, B. D. J Biol NMR 1995, 5, 67–81.
49. Wuthrich, K. NMR of Proteins and Nucleic Acids; Wiley: New York, 1986.
50. Kopple, K. D.; Schamper, T. J. J Am Chem Soc 1972, 94, 3644–3646.
51. Kopple, K. D.; Go, A.; Pilipauskas, D. R. J Am Chem Soc 1975, 97, 6830–6838.
52. Millhauser, G. M. Biochemistry 1995, 34, 3873–3877.